

*Quality of Life and Management of Living Resources*

*Key Action 4 – Environment and Health*

**THz-BRIDGE**

***Tera-Hertz radiation in Biological Research, Investigations on Diagnostics and study on potential Genotoxic Effects***

Contract QLK4-CT2000-00129

**Deliverable D-5**

***Spectral database of selected biological materials and samples***

Submitted by:

USTUTT - M. Dressel, Universität Stuttgart  
UFRANK - W. Mäntele, Johann Wolfgang Goethe-Universität Frankfurt am Main  
TVL - P. Taday, Teraview Limited  
UNOTT - R. Clothier, The University of Nottingham

TABLE OF CONTENTS

1. Spectroscopy of biological materials .....	2
2. Spectroscopic investigations on selected biological samples .....	7
3. Time domain spectroscopy measurements (TDS) at TVL .....	10

# 1. Spectroscopy of biological materials

Aim of this deliverable is to provide a database of the spectral properties in the Far Infrared (FIR) and Terahertz (THz) range for commercial plastic-ware material widely used in biology. Spectroscopic measurements on selected biological samples are also presented. We use a Mach-Zehnder interferometer (see Fig.1) equipped with a series of tunable monochromatic radiation sources to measure the change in power and phase upon transmission through the sample which allows to calculate the complex dielectric constant of the material.

The materials most commonly used as sample for the attachment and growth of cell culture *in vitro* are made from Polyethylene (PE), Teflon (PTFE), Polystyrene (PS) and other non-specified polymer materials such as Thermonox™ (ICN pharmaceuticals, Inc). Prior to using such materials it is important to ascertain their transparency to THz radiation before using them in spectroscopic or irradiation experiment and/or measurements. The group at USTUTT has measured the optical properties of Thermonox™ and tissue culture treated Polystyrene over a large frequency range. Transmission measurements are shown in Fig. 2 and 3. However, it also needs to be born in mind the range of frequencies that are to be employed in apparatus designed for human exposure.

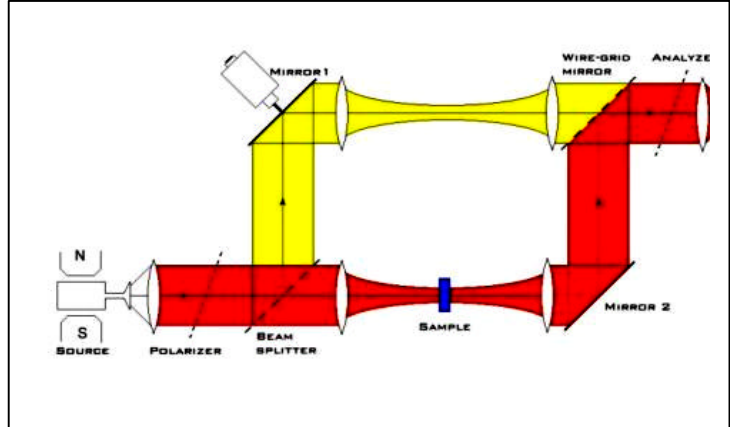


Fig. 1: Mach-Zehnder interferometer utilized in the frequency range from 2 to 40  $\text{cm}^{-1}$ .

Fig. 2: **Thermonox™:**  
Transmission for 0.18 mm path length (left); real and imaginary parts of the dielectric constant (right)

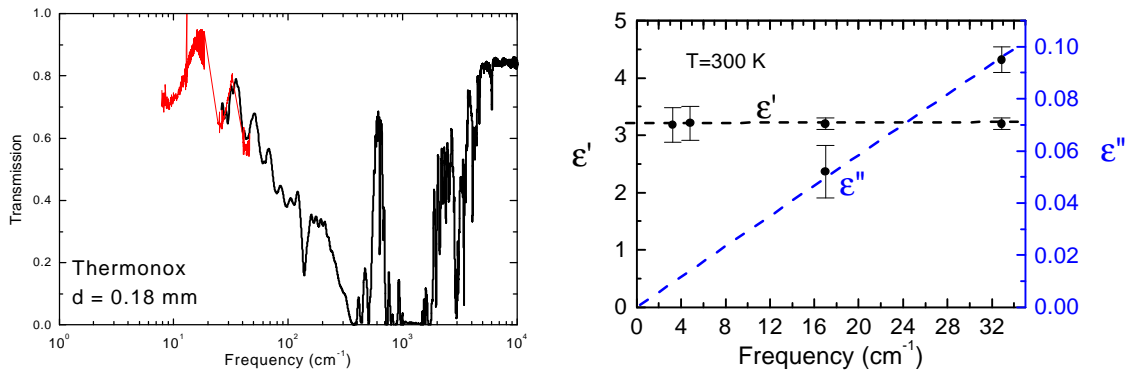
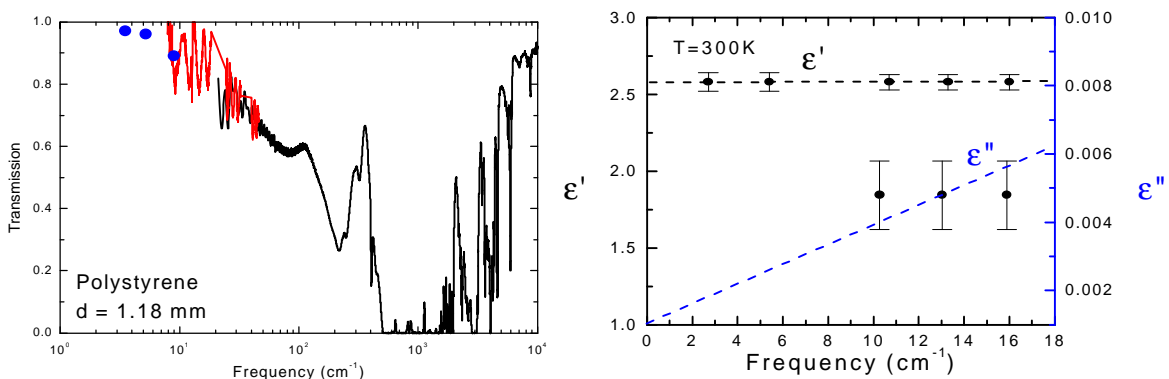


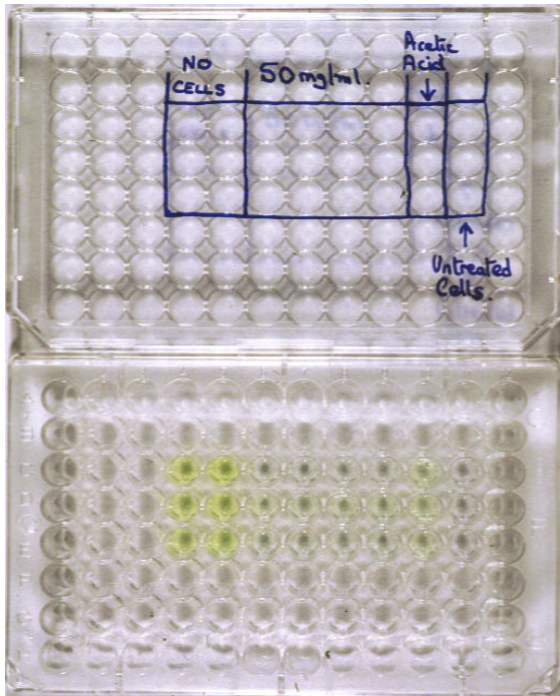
Fig.3: **Polystyrene (NUNC Petri dishes):**  
Transmission for 1.18 mm path length (left); real and imaginary part of the dielectric constant (right)



It is clear from the extensive frequency range measurements that polystyrene is more suitable transmits more, and, therefore, this commonly used material for tissue culture-ware is suitable for our applications due to the lower absorption and the smaller dielectric constant.

The spectra show interference patterns due to multiple reflections from the plane parallel surfaces of the investigated samples. Such interference will be avoided in future experiments using wedge-shaped windows. Plastic materials are difficult to machine very precisely. We also experienced that plastic materials are often too flexible to be operated under differential pressure; it is basically unavoidable that it bends more than can be tolerated for a cuvette.

Typical 96 well tissue culture plate



Typical tissue culture insert, for 24 or 96 well plates

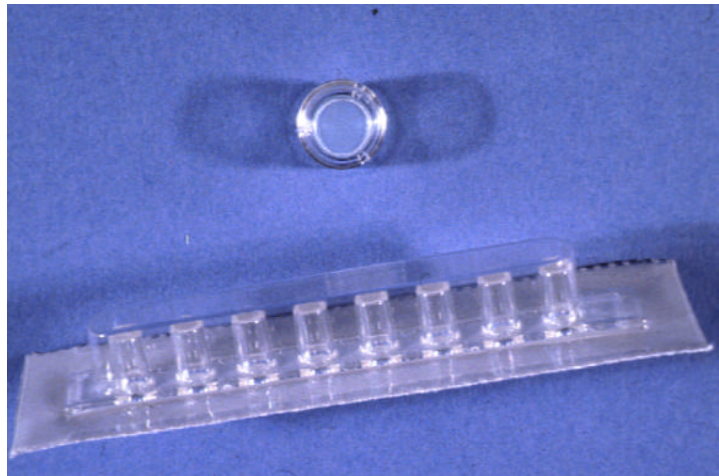


Fig. 4 & 5 Typical tissue plates and inserts.

Further spectroscopic investigations have been performed by USTUTT on other materials, like ZnTe, which may be used as windows of the spectroscopic chamber in the high frequency range between 500 and 10000  $\text{cm}^{-1}$  (15 – 300 THz). The transmission and absorption spectra of ZnTe are reported in Fig.6 and 7 respectively.

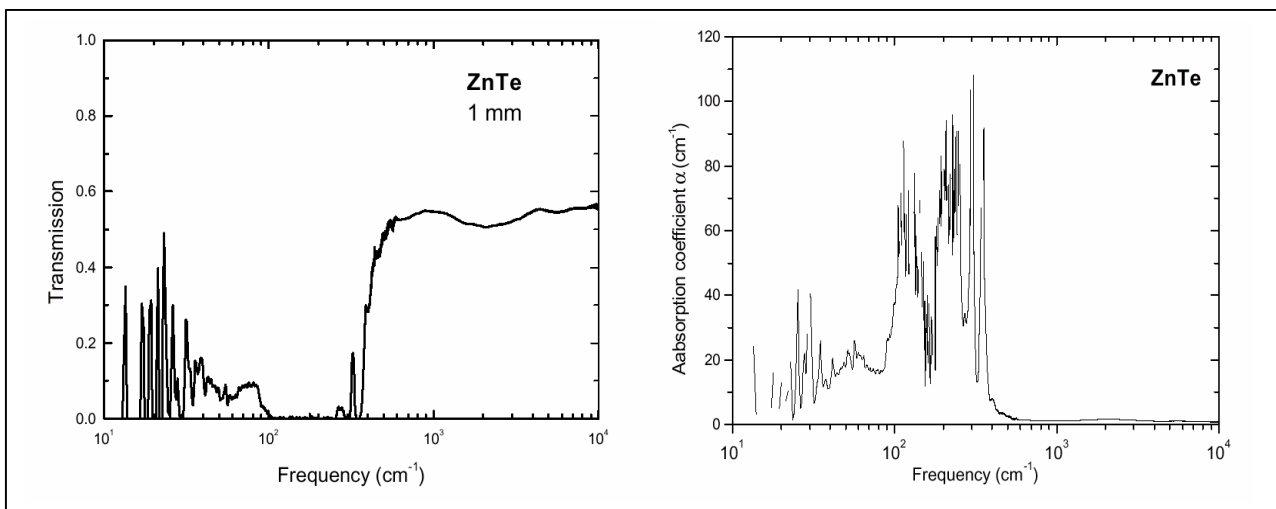


Fig. 6 & 7 Transmission and absorption coefficient of ZnTe .

The other material that was investigated as a possible window material is silicon because it is very stable, chemically inert and easy to machine. The transmission of this is shown in Fig. 8; it very much depends on the doping concentration.

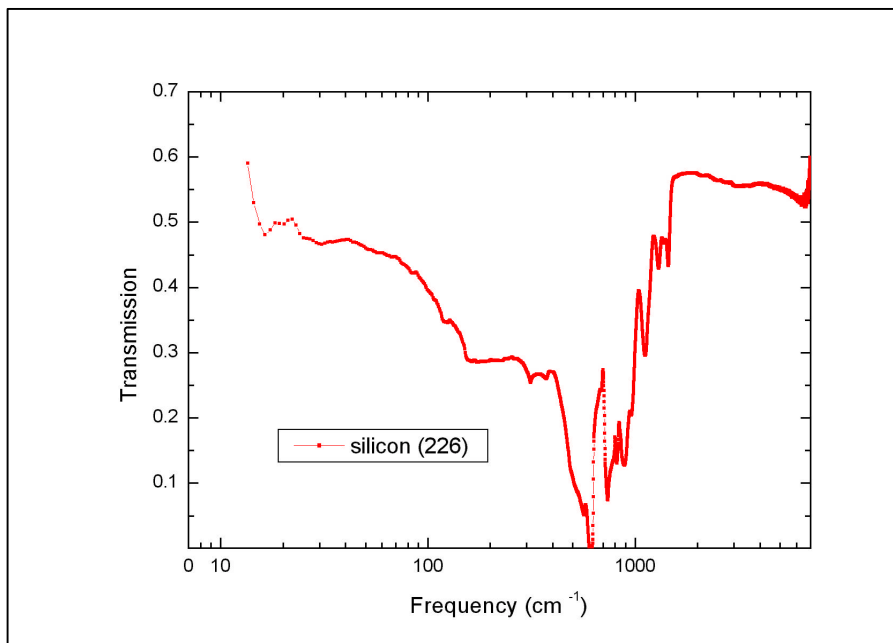


Fig 8. Transmission of a Silicon plate, 2mm thickness, P doped (doping concentration  $4 \times 10^{12}$  atom/cm)

UNOTT has supplied a range of tissue culture plastic-ware and insert membranes (see Figure 4) to USUTT for the evaluation of their transparency to THz radiation. This is to identify those support membranes that will be most suitable to allow significant THz exposure to the basal growing cells in the 3D skin and eye models.. USTUTT has now evaluated a number of membranes and produced spectra for them in their normal ‘dry’ state.

Table 1. The range of insert support membranes tested for THz transmission.

Trade name	Material	Pore size	Thickness	Code name
Anopore	Aluminium Hydroxide	0.2 $\mu$ m and 0.02 $\mu$ m	0.45 $\mu$ m	B2
Millipore PIHA 01250	Mixed Cellulose esters	0.45 $\mu$ m		B3
Millipore PICM 01250	PTFE	0.4 $\mu$ m		B6
Transwell	Polycarbonate	0.4 $\mu$ m, 3.0 $\mu$ m, 8.0 $\mu$ m	19 $\mu$ m, 17 $\mu$ m, 12 $\mu$ m	PC
Falcon	PET track-etched membrane	0.4 $\mu$ m		B4
Falcon	Polycarbonate	3.0 $\mu$ m	17 $\mu$ m	B5

The preferred Anopore membrane, made of aluminum hydroxide with 50% porosity, was shown to markedly restrain THz transmission, particularly the one with 0.02 $\mu$ m pore size. Further studies on the most THz opaque membranes needs to be undertaken to determine the effects of water retention in the pores and or the material, under normal culture conditions. In addition, for the Millipore PICM membranes a extra cellular matrix coating (ECM) will be required to allow for cell attachment, thus this coating on the membrane in the presence of aqueous medium will also require assessment. In addition those parts of the spectrum which relate (a) to those defined in the project i.e. from 100 GHz up to 20 THz, and (b) those related to the output of the machine used for dermatology, i.e. from 1 – 10 THz, should be examined. This work is now underway and will be used to identify the best membrane upon which to culture the 3D models and/or confluent monolayers. Once the membrane has been identified, its THz transparency when wet with medium will be assessed along with any additional matrix coating, required to ensure cellular attachment.

These membranes are employed to support the cells above the normal tissue culture wells such that the cells can be fed with medium from below. Thus, the insert membranes are held above the lower surface of the well upon which the cells are normally grown. The inserts either have small feet to hold them up, or hang from the top of the well. Since the medium is aqueous there will be considerable absorption of the THz by this layer of medium. Hence, if to be used, the cultures will require to be exposed to the THz in well devoid of medium (Fig. 9).

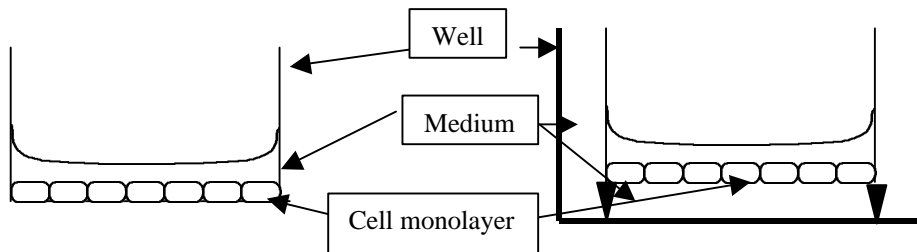


Fig. 9 Monolayer culture of cells on the base of the well c.f. with cells on an insert support membrane.

USUTT tested the transmission properties of a range of tissue culture plastic-ware and insert membranes used by the group at the University of Nottingham (See Table 1). From the spectra it is apparent that some are highly transparent in the range of THz frequency, which make them suitable to consideration. The Millipore membrane PICM 01250, the PTFE membrane without ECM coating, has the highest transmission being approximately 0.9 in the frequency range from 50 to 400 wave numbers. The poorest transmission is exhibited by Millipore PIHA01250. However, it should be noted that these were tested under dry conditions.

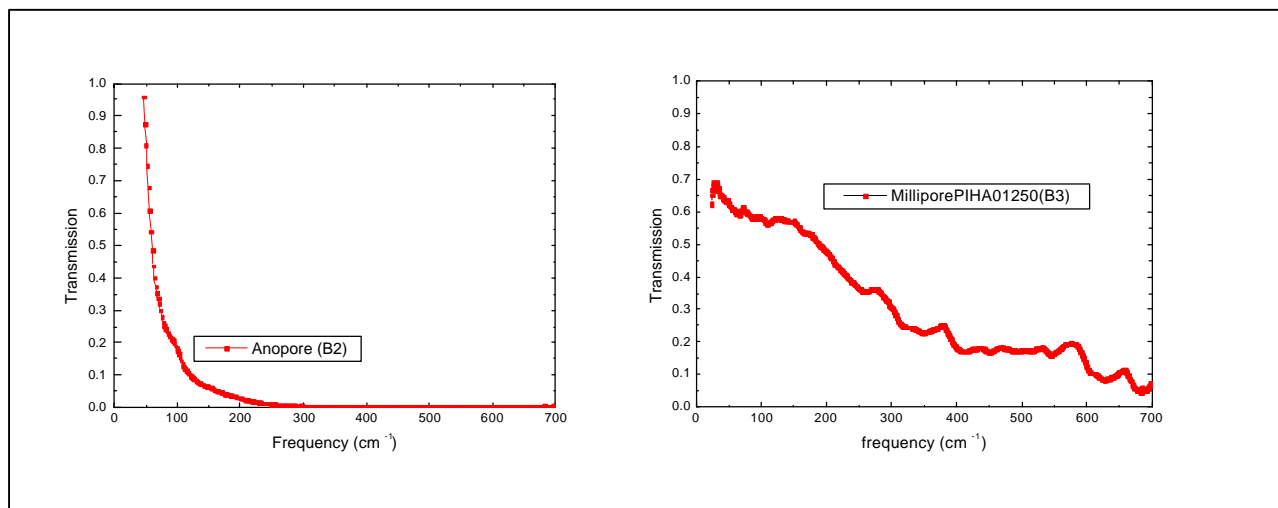


Fig. 10 Membranes transmission (B2, B3)

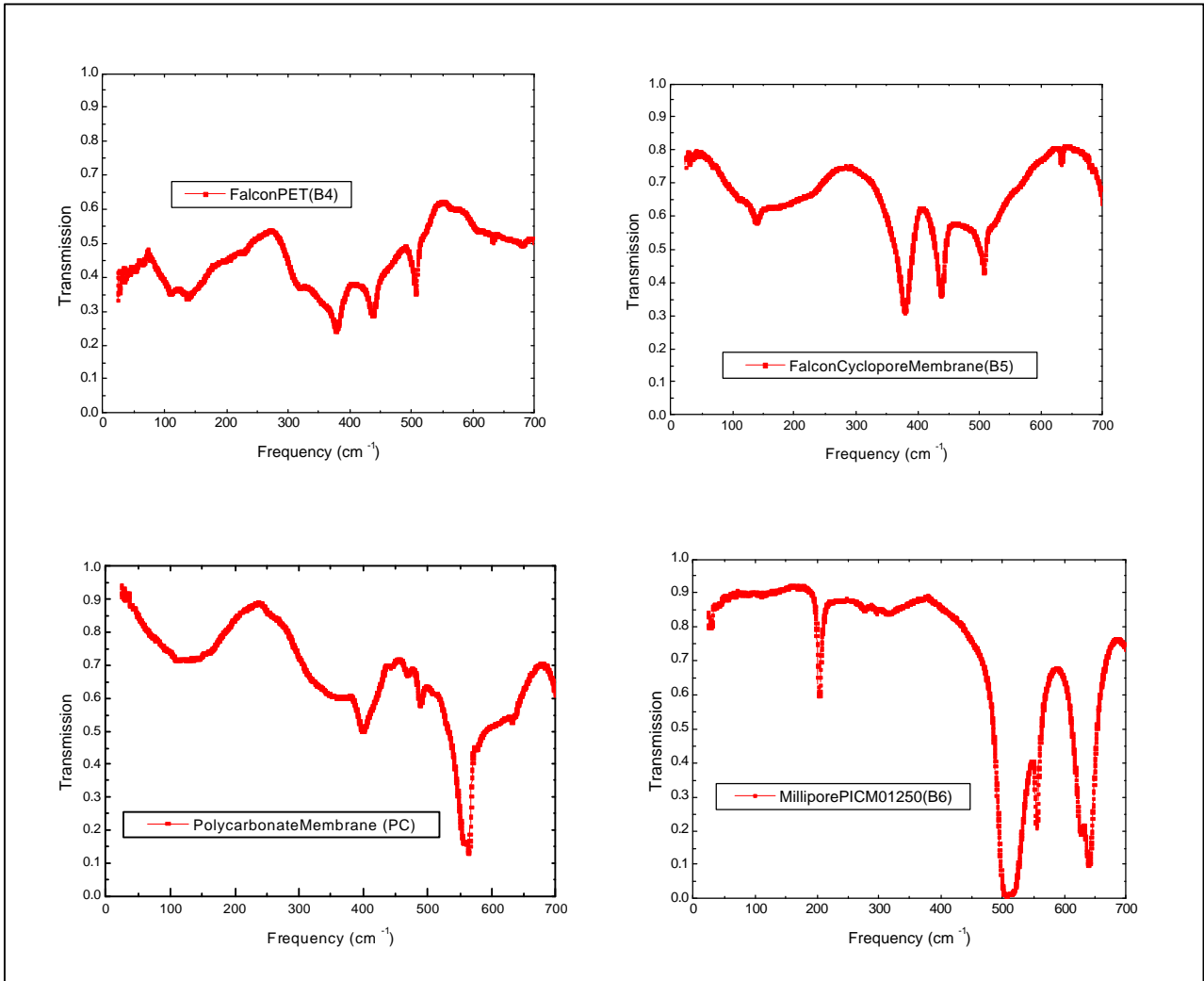


Fig 10 (cont. from page 5 ) (membranes B4, B5, B6 and PC)

## 2. Spectroscopic investigations on selected biological samples

Starting in fall 2001 USUTT performed experiments on biological systems in the submillimeter wave range using backward wave oscillators as tuneable radiation sources.

In order to improve the spatial resolution in such measurements a THz near-field microscope was developed, which allows to perform reflection measurements on spot sizes down to  $\lambda/100$ . As displayed in Fig. 11, the set up consists of a near-field unit (1.1) mounted rotatable by 90 degrees (1); one axis is used for a quasi-optical spectrometer(2), and the second by a confocal microscope(3) for distance control. The core part of the near-field spectrometer is a small pinhole(1) which is drilled in a copper foil (thickness 1 to 10  $\mu\text{m}$ ) with diameter as small as 1  $\mu\text{m}$  and which generates the evanescent submillimeter wave. Behind the pinhole sits the sample (4) which can be translated relatively to the pinhole by three linear piezo-motors (3) are used. These motors are based on stink and slip motion with a step size of 40 to 400 nm. There is a fourth motor for moving the sample and pinhole together, which is required for the distance control via the confocal microscopy. The distance between pinhole and sample is modulated  $\pm 70 \mu\text{m}$  with high frequencies (about 1 kHz) by an additional piezo-electric bender in order to using look-in technique for data acquisition. The near-field unit is installed on an rotatable frame for performing THz measurements on the one side and the distance control via the confocal microscope on the other side.

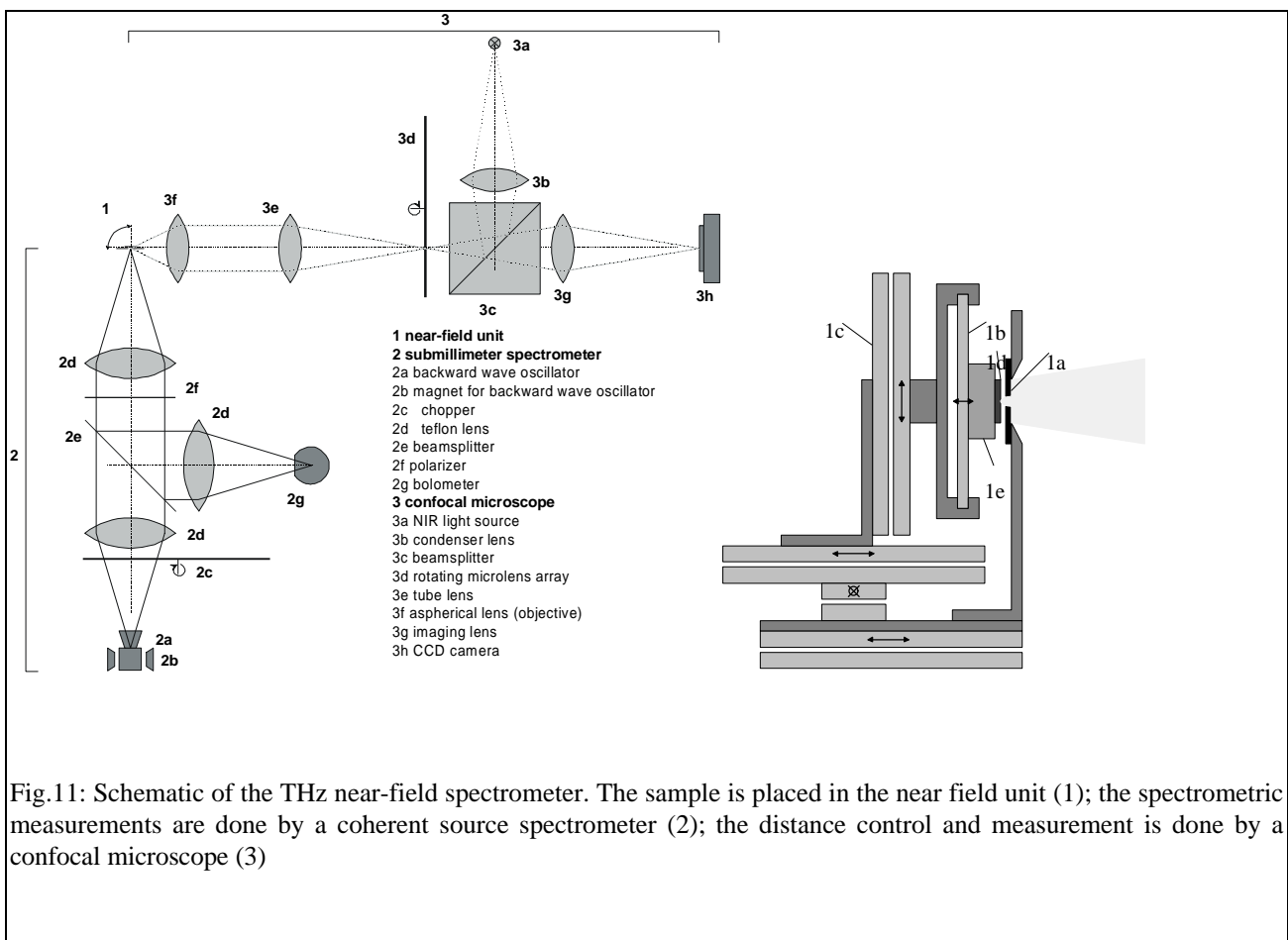


Fig.11: Schematic of the THz near-field spectrometer. The sample is placed in the near field unit (1); the spectrometric measurements are done by a coherent source spectrometer (2); the distance control and measurement is done by a confocal microscope (3)

USUTT checked the transmission in the submillimeter domain through several biological samples, among these chicken bone and ham. The measured values are shown below. (Fig. 12 and 13).

Fig 12: Ratio of reflected power of chicken bone

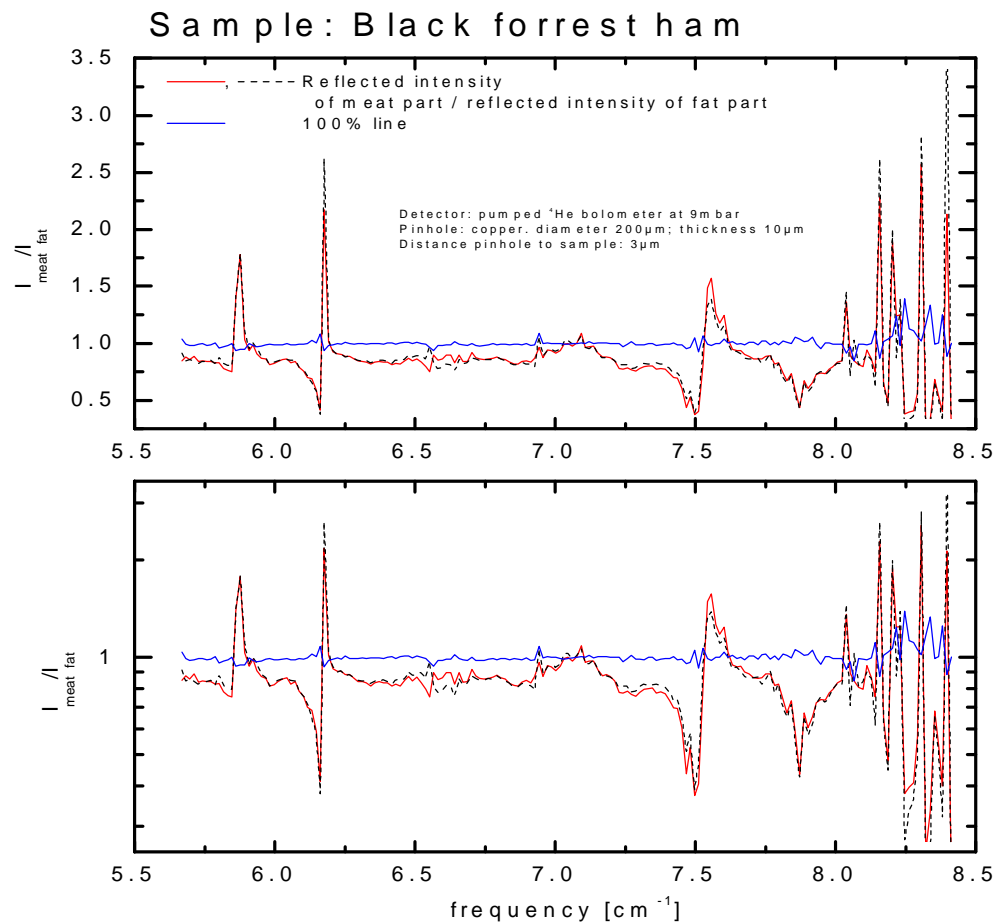
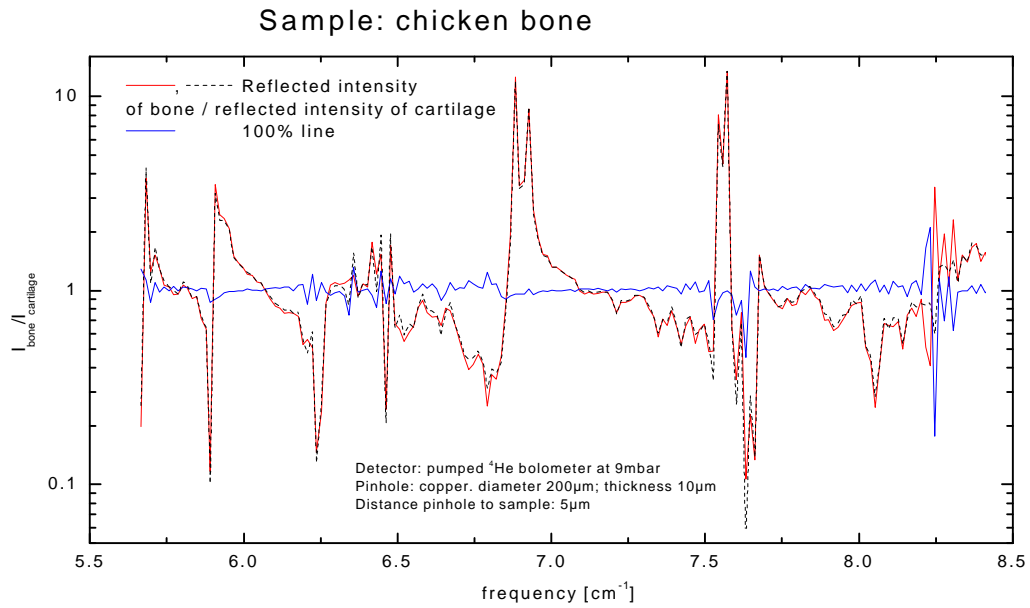


Fig. 13: The solid line shows the reflectivity of the meat part normalized of the reflectivity of the fat part of Black Forrest ham averaged on three points each.

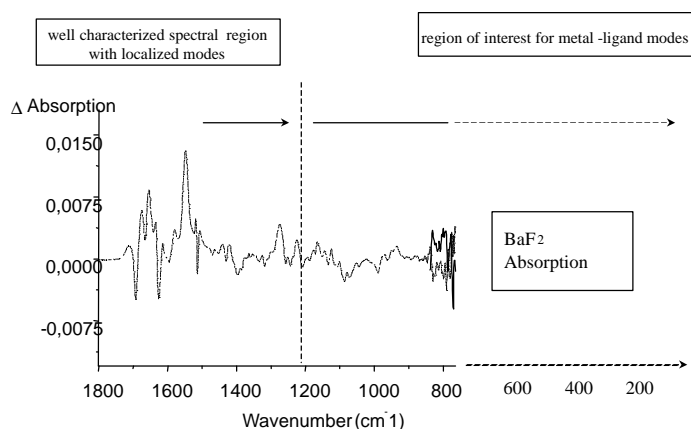
For the interpretation of these spectra a study of the spectral properties of some basic proteins and aminoacids is necessary. In this respect USTUTT wants to dedicate some time to characterize the behavior of aminoacids in interaction with THz radiation. The sharp peaks that appear on the spectra could be very useful in imaging applications, since they can be exploited to enhance contrast between different tissues. Part of these results were presented at the BISAT2001 Conference on biological imaging with THz radiation held in Leeds (UK) in December 2001 and will be published in the journal "Physics in Medicine and Biology". The next step in the project is to determine the transmission characteristics for samples like blood and its individual constituents. In parallel measurements on heme-containing proteins (cytochrome c, hemoglobin) will be carried out.

Model systems for FIR spectroscopy were selected by UFRANK in order to provide correlations between structural and spectroscopic properties. The models selected so far include:

- Individual amino acids. These compounds will be analyzed in solution and under controlled buffer conditions in order to ensure defined protonation states. In addition, analysis of amino acids in tripeptides of the general form GLY-X-GLY, with X being the amino acid under investigation, will be performed. This procedure ensures standard contributions from the peptide bond and the carboxy/amino terminal side for all amino acids and allows the investigation of side chain modes;
- Small peptides and proteins of medical relevance. These models will be analyzed for the FIR contributions from the respective secondary structure.
- Water soluble proteins with a metal center (heme and/or copper), such as the small blue copper protein azurin and cytochrome *c* as paradigm of a heme protein. From these investigations, the spectral attribution of metal-ligand modes is expected. Most of these proteins are redox-active and will be investigated with RIDS spectra to investigate functionally relevant modes.
- In collaboration with a medical research group as a subcontractor of UFRANK, full blood samples (EDTA stabilized), blood platelet samples, white cells and plasma/serum samples will be analyzed

#### Preliminary reaction-induced IR difference spectra (RIDS) below 1000 cm<sup>-1</sup>

As an attempt to cover the spectral region below 1000 cm<sup>-1</sup>, the IR spectroelectrochemical cell was



equipped with BaF<sub>2</sub> instead CaF<sub>2</sub> windows. This extends the spectral range to below 800 cm<sup>-1</sup>. The spectrum in Fig.14 shows redox-induced FT-IR difference spectra of cytochrome *c* in the range thus accessible. The symmetry of the signals due to the oxidizing and to the reducing step, resp., even in the region below 1000 cm<sup>-1</sup>, indicates modes active in the redox transition. We consider this as highly encouraging for the extension of these studies to the 1000 cm<sup>-1</sup> to 400 cm<sup>-1</sup> range in the UFRANK group and to frequencies below in collaboration with the USTUTT group.

Fig.14 FT-IR difference spectra of cytochrome *c*

### 3. Time domain spectroscopy measurements (TDS) at TVL

A set-up for Time Domain Spectroscopy (TDS) measurements has been developed at TVL and is shown in Fig.15.

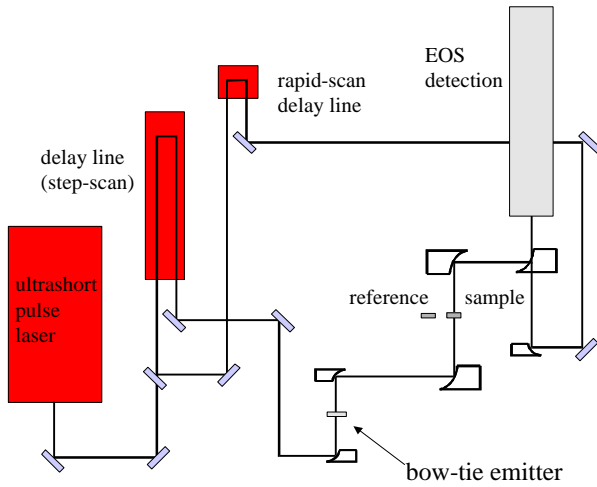


Figure 15: a) Schematic diagram of set-up to measure high bandwidth emission from *p-i-n* sources. b) Time-domain spectrum of the response from the *p-i-n* photodiode. c) FFT of figure 1(b). (Blue trace in dry nitrogen, red trace in air) The sharp feature at 8.8 THz is due to the LO photon vibration in GaAs.

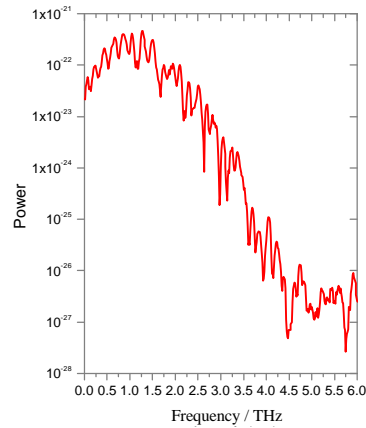


Figure 16: Typical response from the bow-tie emitter used in time-domain spectroscopy.

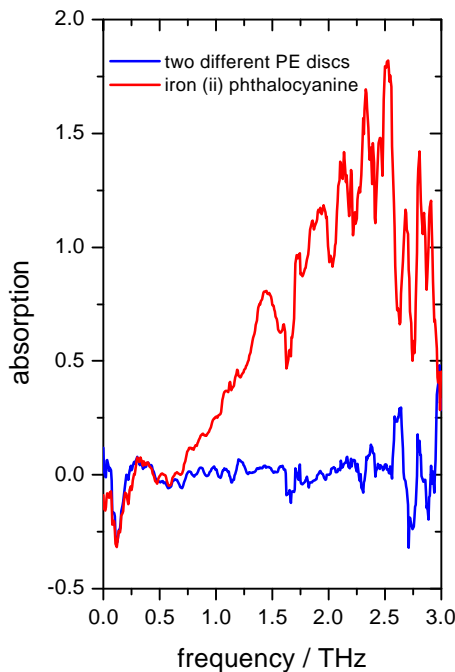


Fig. 17: The THz spectrum of iron (ii) phthalocyanine (red trace). The blue trace shows the THz spectra of two different polyethylene (PE) discs normalised to each other.

For these experiments a Coherent Vitesse Ti:Sapphire laser and a TeraView designed bow-tie emitter were used. The spectrum obtained from the emitter is shown in figure 16. Electro-optic sampling

(EOS) with a thin (200  $\mu\text{m}$ ) ZnTe detector was used to detect the THz radiation. Two THz-spectra are normally obtained- a sample and a reference signal.

As an example of THz spectrum we used iron (ii) phthalocyanine. The iron (ii) phthalocyanine was mixed with a 50/50 mixture weight:weight with polyethylene. The mixture was compressed in a mechanical press to a load of 2-tons in a 13-mm disc. The THz absorption spectrum at room temperature is shown in figure 17. At this stage no attempt has been made to assign the features observed in the spectrum, but the feature at about 50- $\text{cm}^{-1}$  maybe due a vibration involving the metal ligand bond between the iron atom and the phthalocyanine molecule. Assignment of this band can be confirmed by isotope substitution of the iron atom. Many of the sharp features observed in the spectra above 2-THz or 60- $\text{cm}^{-1}$  are due to water vapour. We are currently redesigning the apparatus to remove water vapour from the system. Also, shown in figure 17 is the spectrum obtained when normalising between two different polyethylene discs.

More work will be undertaken to explore the underlying reason for the gradient in the spectrum from 0.5 to 3 THz. This could be due for example due to the increased scatter of THz radiation from particle size in the polyethylene disc loaded with the test molecule or it could be due some general broad absorption underlying the whole region.

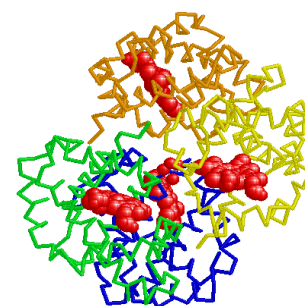
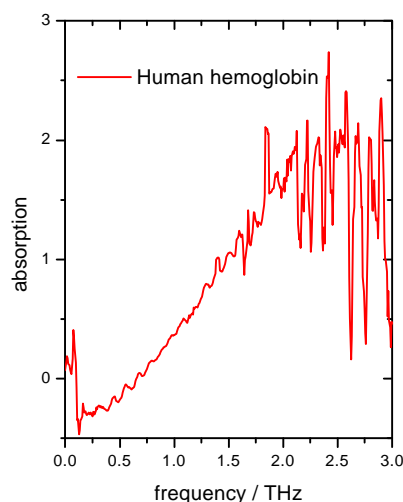


Fig. 18 Human emoglobin protein and spectrum

In figure 18 we shows the typical THz spectrum obtain obtained from dried human hemoglobin. The sample was prepared in a similar way to the iron (ii) pthalocyanine. This time no features are observed in the spectrum. But, there is still a general broad increase in absorption over the range 0.5 to 2.5 THz.

Figure 19 shows the THz spectrum for melanin. Again, the spectrum is broad and featureless. More recently we have obtained the THz spectrum of uric acid, figure 20, in this spectrum we observe a number of very sharp features, most notably at 47.6 and 79.1  $\text{cm}^{-1}$ . These vibrations could be due to a general umbrella motion in the ring structure of the molecule. We plan to undertake some local-mode calculations to confirm the assignment of these bands.

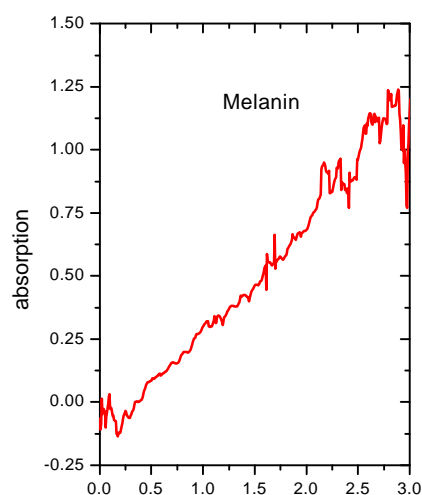


Fig. 19: The THz spectrum of melanin

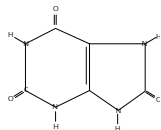
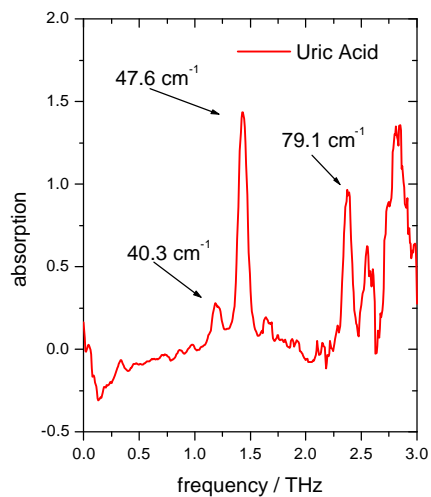


Fig. 20: The THz absorption spectrum of uric acid

The database of molecules of interest to irradiation studies and to Terahertz imaging techniques will be extended with the Deliverable D-12 “*Database of relevant frequencies to provide high contrast in imaging applications*”. To-date all this work has been achieved with dry samples we will progress onto liquid samples using the cells designed and manufactured by partner UFRANK.